

A Strategic Approach for 2D Texture Analysis using DTCWT, SWT and GLCM

C. Rama Mohan¹, S. Kiran², Vasudeva³

¹(Research Scholar, Department of CSE, VTU, Belgaum, Karnataka, India)

²(Department of CSE, YSREC of YVU, Proddatur, Andhra Pradesh, India)

³(Department of ISE, NMAM Institute of Technology, Nitte, Karnataka, India)

Corresponding Author: ramamohanchinnem@gmail.com

To Cite this Article

C. Rama Mohan, S. Kiran, Vasudeva "A Strategic Approach for 2D Texture Analysis using DTCWT, SWT and GLCM", *Journal of Science and Technology*, Vol. 07, Issue 02, Mar-April 2022, pp.:195-209.

Article Info

Received: 18-03-2022

Revised: 02-04-2022

Accepted: 15-04-2022

Published: 21-04-2022

Abstract: Nowadays, 2D imaging techniques have gone through several stages of development in 2D sensor technologies. This probes greater interest in the 2D image feature extraction and classification techniques. One of the main features of 2D image are texture content which is very enthusiastic to study. The proposed strategy is to extract and analyse of texture content of 2D image. In this strategy Dual Tree Complex Wavelet Transform (DTCWT) and Stationary Wavelet Transform (SWT) with Principal Component Analysis (PCA) is implemented to extract the features of the 2D images especially texture content for further analysis. The texture content is analysed with Gray-Level Co-Occurrence Matrix (GLCM) based method which increase the precision of the data obtained which causes better result.

Key Word: Texture Analysis, Feature Extraction, Gray-Level Co-Occurrence Matrix, Dual Tree Complex Wavelet Transform, Stationary Wavelet Transform, Principal Component Analysis

I. Introduction

Image feature extraction and Analysis domain as caused enthusiasm in the researchers and developers as there is development in the domain and it's wide range of applications [1-3]. The development in this domain becomes mandatory as it's uses increases day by day [4-13].

Image fusion is a process in which we gather all the dominant information from multiple images which are obtained under different circumstances. This gathered information is incorporated into fewer images, usually it a single image in most cases. These images obtained by the image fusion are more accurate and contains precised and dominant information than any single source from where these images are obtained [14-15].

Images analysis is a process of extraction of meaningful information from images [16]. It can be used on simple to sophisticated images. It is quantitative and qualitative characterization of 2D or 3D images. It is mainly obtained from the contrast, dynamic range, spatial resolution, noise and artifacts of images. In image analysis there exists texture analysis [17-18]. Texture analysis is referred as the characterization of regions in an image by their texture content.

Texture analysis is divided into four stages: texture segmentation, texture synthesis, texture classification, and texture shape [19-21]. To achieve texture analysis, local statistical measures such as entropy, the range of pixels in the image or the standard deviation of pixels in the image are used. There are various qualities of an image that may be measured with hardness, brittleness, spread-ability, adhesiveness, tensile strength, and extensibility.

The subject of evaluating the relative performance of different texture analysis approaches has gained a great deal of interest in the scientific literature in recent years. A global measurement of a particular algorithm's performance is nearly impossible due to the nearly limitless number and variety of textures that can be created, as well as the difficulty in identifying the very nature of texture itself. Instead, a relative measure may only be obtained within the context of a certain set of images or a particular application. In order to make such comparisons easier, various texture databases have been compiled, which are frequently utilized in the scientific community today.

II. Literature Survey

In recent years, several strategies were proposed and developed by various scholars in texture analysis. One of a work accomplished in Ayushman Ramola et al [22]. In this work four systematical methods for texture analysis were considered. These methods includes GLCM, LBF, ACF and histogram pattern. From statistical study of these methods they concluded that GLCM is performed well for texture analysis when compared to other proposed methods. LBP is good for object recognition. ACF is also can be used for texture analysis but the results obtained in this method is not commensurable for result obtained by GLCM.

Taiki Orima and Isamu Motoyoshi [23] suggest a strategy for texture analysis and synthesis. In this strategy visual evoked potentials were exploited for analysis and synthesis of natural texture perception. In this method VEP signals are utilized to extract the texture from dynamics visuals. As VEP signal scrupulously associated with texture. This strategy utilized this signal for texture analysis.

Laurentius O. Osapoetra et.al [24]. proposed a strategic approach. There approach exploited the QUS spectral parametric image to texture extraction and analysis. In this method texture extraction and analysis is implemented on breast lesion QUS spectral parametric digital images. This strategy classified texture of various part of breast lesion with greater than 90% precision. From this work a conclusion is obtained that QUS spectral parametric images for texture analysis out perform most of various images which are exploited in various strategies.

Xin Zhang et al. [25] resolved the problem of extracting texture features from images, and a direction measure statistic based on the directionality of image texture is built. This article proposes a novel texture feature extraction approach based on the direction measure and a GLCM fusion algorithm. Applying the GLCM, this method extracts an image's texture feature value and incorporates a weighting factor introduced by the direction measure. Images were classified using a Support Vector Machine (SVM) using the direction measure and Gray Level Co-Occurrence Matrix fusion technique for the high-resolution images. In order to evaluate the classification outcomes, we used both qualitative and quantitative methodologies. Using the fusion approach to extract texture features enhanced image identification and classification accuracy greatly, according to the testing results.

According to Zhi-Kai Huang et al [26], PCA fusion-based GLCM features in image segmentation can be used to segment textures using principal component analysis (PCA) fusion. First, four of Haralick's most common characteristics are calculated. In the second step, we use principal component analysis to turn the four features retrieved data into four principle components. Then, using the weighted average rule based on PCA, select the fused coefficient. Fusion image has finally been processed using a method that uses k-means clustering. The results of the experiments show that the proposed method is successful and can reach desirable precision. On the basis of the PCA weighting methods studied in this work, a new idea has been proposed: PCA fusion rules will be utilized to segment images. As a drawback, finding an acceptable number of features to produce good segmentation often necessitates a trial-and-error procedure; at the same time, the computation time is high for larger images. As a result, future research into the optimum features for these scenarios is a possibility.

III. Material and Methods

Grey Level Co-occurrence Matrix is systematically proposed strategy by Robert Haralick et al in 1973 to analysis the texture of image which considers the spatial relationship of pixels. It is also known as gray-level spatial dependence matrix. It mainly works on the principle based on the spatial distance between pixels in an image. It is

widely utilized in texture analysis domain. In this paper we utilize GLCM to analysis the texture of a fusion image which is generated by DTCWT and SWT with modified PCA. The block diagram of proposed methodology is shown in Fig. 1.

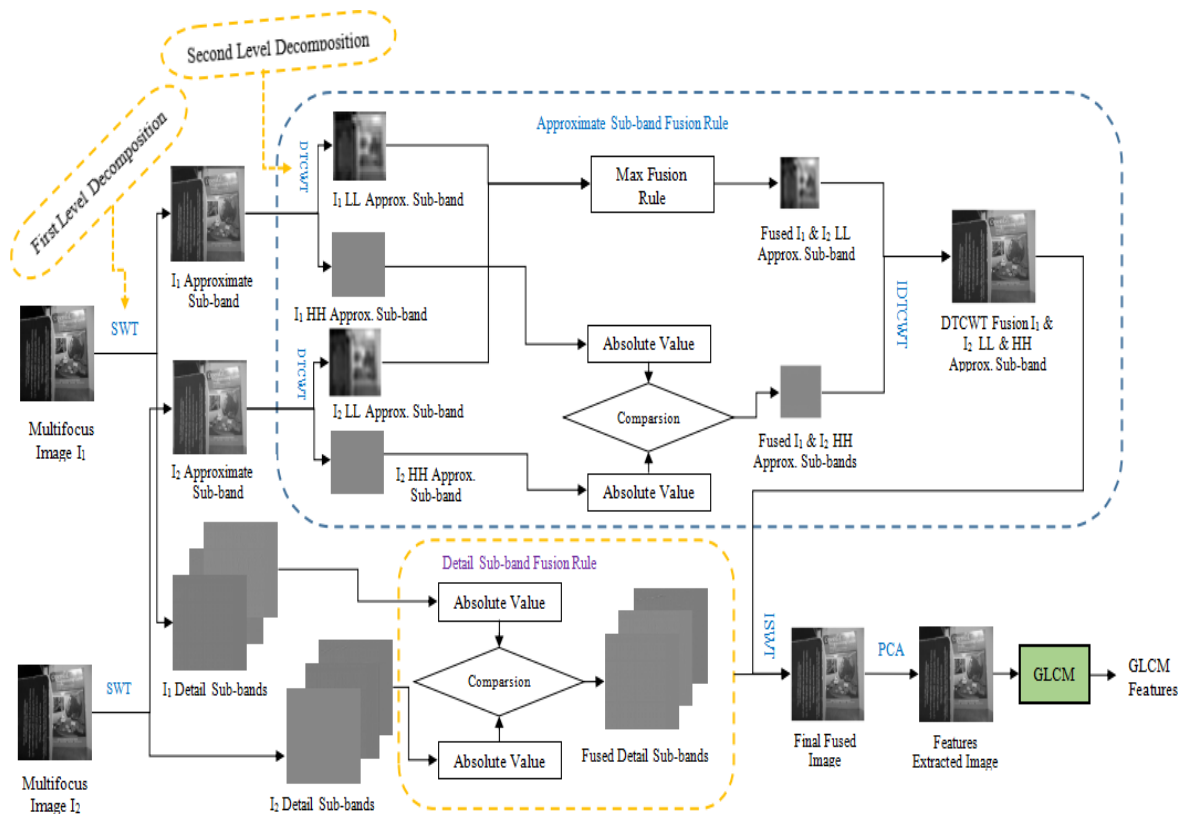


Fig. 1. Flow Diagram of the Proposed Method

The detailed description of above represented flow diagram is given below:

1. Read multi-focus images.
2. Apply first level of decomposition for the given multi-focus images using SWT which divides the given input images into two types of sub-bands as approximate sub-bands and detail sub-bands.
3. In the second level of decomposition implement DTCWT for approximate sub-bands which further divide the data of images into LL components and HH components.
4. Implement max fusion for LL approximate sub-bands which are obtained from DTCWT to generate fused approximate sub-band of LL components.
5. For remaining HH approximate sub-bands of DTCWT compare the intensities of these two sub-bands which ever have maximum intensity among given sub-bands is consider for final HH approximate sub-band.
6. Implement IDTCWT on LL and HH fused sub-bands which generates fused sub-band of LL and HH approximate sub-band.

7. In the other hand first level decomposed detailed sub-bands are compared individually which ever intensity is maximum that is to be considered for final detailed sub-band.
8. To generate final fused image apply inverse SWT for DCTWT fused image and final detailed sub-band.
9. Implement principle component analysis to extract more feature from final fused image.
10. The texture analysis with contrast, orderliness and statistical group are analyzed with GLCM.

IV. Result and Discussion

In order to estimate performance of symmetrical GLCM it's necessary to evaluate statistical values with respect to image measures are represented with two types first order and second order [18]. When statistics of texture of image need to evaluate first order statistics like brightness contrast are not useful because there are directly derived from the pixels. Instead of first order statistics, second order statistical measures are used to define the texture image. The brief description each second order statistics measures given below.

Contrast: The variation in brightness between light and dark region of an image is called contrast which is evaluated by the given

$$\text{contrast} = \sum_{n=0}^{255} \sum_{m=0}^{255} (n - m)^2 p(n, m)$$

Dissimilarity: Variations in an image from pixel to pixel is called dissimilarity which is evaluated by the given

$$\text{Dissimilarity} = \sum_{n=0}^{255} \sum_{m=0}^{255} |n - m| p(n, m)$$

Homogeneity: Similarity in an image from pixel to pixel is known as homogeneity which is evaluated by the given

$$\text{Homogeneity} = \sum_{n=0}^{255} \sum_{m=0}^{255} \frac{p(n, m)}{1 + (n - m)^2}$$

Angular Second Moment: The uniformity of distribution of gray-level in an image is known as angular second moment which is evaluated by the given

$$\text{Angular second moment} = \sum_{n=0}^{255} \sum_{m=0}^{255} [p(n, m)]^2$$

Max probability: The maximum value of probability of occurrence of required contrast level is known as max probability which is evaluated by the given

$$\text{Max probability} = \text{Maximum elements in NGLCM}$$

Entropy: Number of bits are needed to encode the data present in a image is known as entropy which is evaluated by the given

$$\text{Entropy} = \sum_{n=0}^{255} \sum_{m=0}^{255} -P(n, m) \log_e [p(n, m)]$$

Energy: Minimization problem or maximization problem present in image processing is called energy which is evaluated by the given

$$\sqrt{\sum_{n=0}^{255} \sum_{m=0}^{255} [p(n, m)]^2}$$

GLCM Mean: GLCM mean is evaluated by the given

$$\mu = \sum_{n=0}^{255} \sum_{m=0}^{255} np(n, m) = \sum_{n=0}^{255} \sum_{m=0}^{255} mp(n, m)$$

GLCM Variance: GLCM variance is evaluated by the given

$$\sigma = \sqrt{\sum_{n=0}^{255} \sum_{m=0}^{255} (i - \mu)^2 p(n, m)}$$

GLCM Correlation: GLCM correlation is evaluated by the given

$$\text{GLCM correlation} = \sum_{n=0}^{255} \sum_{m=0}^{255} p(n, m) \frac{(n - \mu)(m - \mu)}{\sigma^2}$$

In order to examine the efficiency of the suggested strategy, 32 test images (i.e., source and fused images) are employed in the trials. Figs. 2 and 3 illustrates the test images.

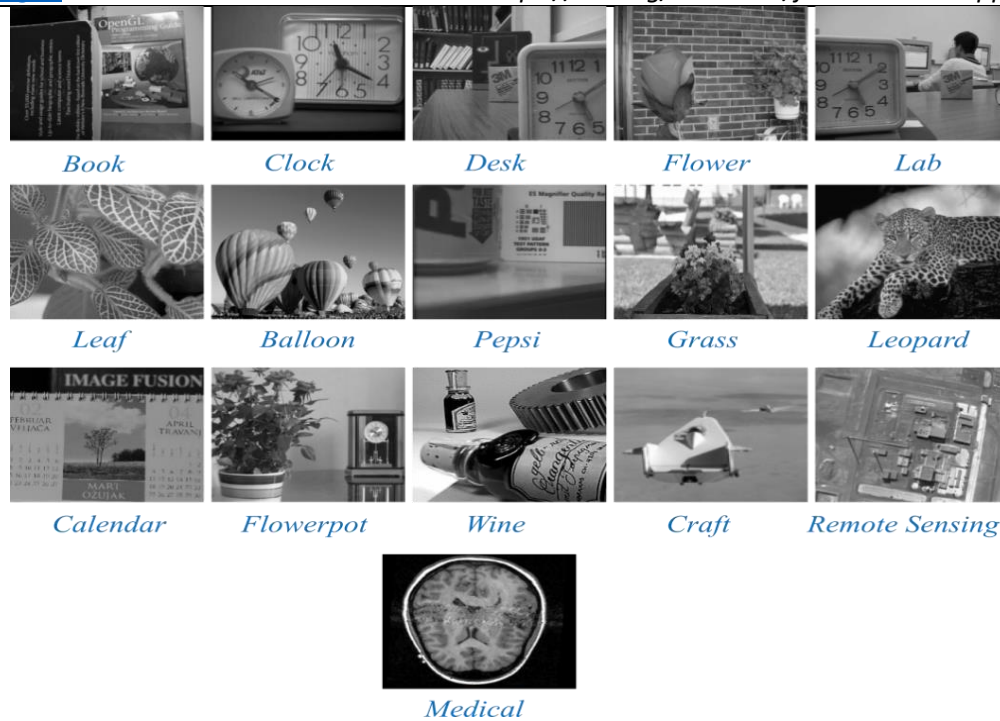


Fig. 2. The source images used in experiments

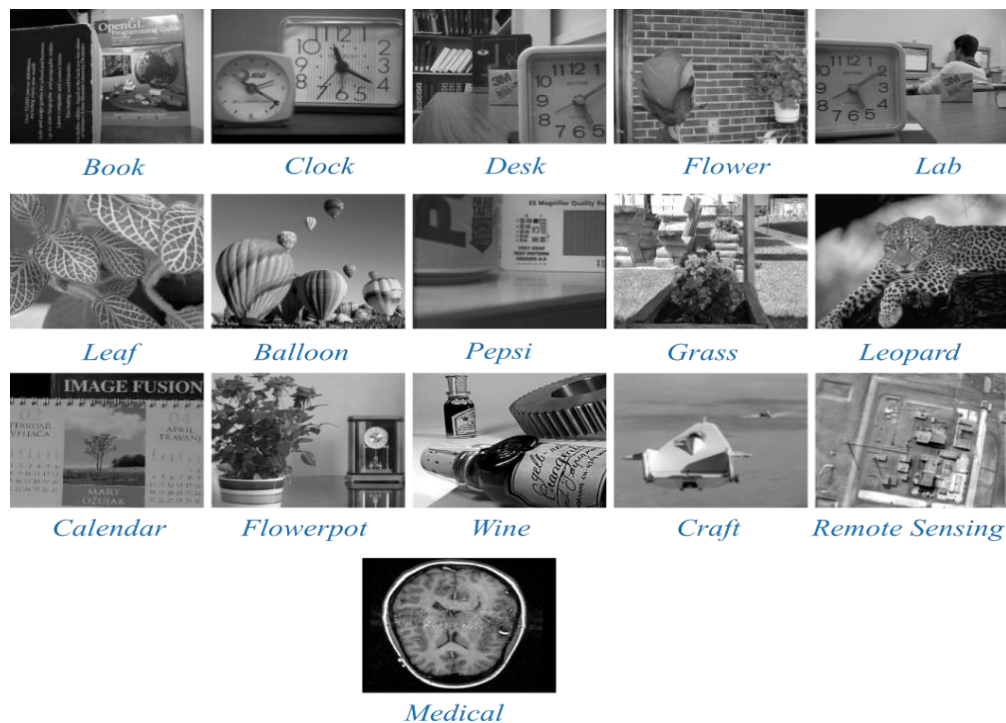


Fig. 3. The fused images (SWT+DTCWT and PCA) used in experiments

In this proposed work, texture measures are computed for 32 images. The entire analysis of the test image along with its ground truth is shown in the table.

Table I. Contrast, Dissimilarity, and Homogeneity of Contrast Group for Thirty Two Test Images

Image	Contrast Group		
	Contrast	Dissimilarity	Homogeneity
Ground Truth Image (Book)	317.694818	9.118444	0.329186
Fused Image (Book)	521.84884	10.650125	0.31861
Ground Truth Image (Clock)	69.940522	4.560595	0.397381
Fused Image (Clock)	69.336855	4.602927	0.375723
Ground Truth Image (Desk)	190.793336	6.571741	0.333574
Fused Image (Desk)	194.864379	6.786805	0.305584
Ground Truth Image (Flower)	453.727218	12.789723	0.149427
Fused Image (Flower)	455.882971	12.947193	0.143241
Ground Truth Image (Lab)	154.727693	5.562152	0.439042
Fused Image (Lab)	158.918633	5.750118	0.402059
Ground Truth Image (Leaf)	701.966347	17.384476	0.342027
Fused Image (Leaf)	728.923673	19.188096	0.082348
Ground Truth Image (Balloon)	360.337136	7.862955	0.337314
Fused Image (Balloon)	361.779209	7.889395	0.335340
Ground Truth Image (Pepsi)	181.090146	6.569759	0.231643
Fused Image (Pepsi)	187.054752	6.977118	0.205577
Ground Truth Image (Grass)	404.550274	12.634781	0.137621
Fused Image (Grass)	1094.657618	21.271122	0.106026
Ground Truth Image (Leopard)	354.665139	11.013230	0.246694
Fused Image (Leopard)	356.996424	11.058345	0.243547
Ground Truth Image (Calendar)	600.197174	12.051206	0.293438
Fused Image (Calendar)	626.927555	12.347437	0.264968
Ground Truth Image (Flowerpot)	480.782414	11.239805	0.287468
Fused Image (Flowerpot)	491.176493	11.433887	0.263965
Ground Truth Image (Wine)	1848.368558	23.127793	0.318342
Fused Image (Wine)	1993.264815	26.184882	0.116980
Ground Truth Image (Craft)	148.198726	4.744195	0.398249
Fused Image (Craft)	151.477948	4.973854	0.364210
Ground Truth Image (Remote Sensing)	247.677422	8.962290	0.180053
Fused Image (Remote Sensing)	297.757155	10.538118	0.150218
Ground Truth Image (medical)	585.519569	10.930719	0.419862

<i>Fused Image (medical)</i>	637.528258	12.206521	0.220456
------------------------------	------------	-----------	----------

Table II. ASM, Max Probability, Entropy, and Energy of Orderliness Group for Thirty Two Test Images

Image	Orderliness Group			
	ASM	Max Probability	Entropy	Energy
Ground Truth Image (Book)	0.001463	0.014869	3.569683	0.038243
<i>Fused Image (Book)</i>	0.001061	0.010955	3.613156	0.03257
Ground Truth Image (Clock)	0.001866	0.026145	3.409659	0.043198
<i>Fused Image (Clock)</i>	0.001363	0.019784	3.439152	0.03692
Ground Truth Image (Desk)	0.000869	0.010376	3.517338	0.029471
<i>Fused Image (Desk)</i>	0.000670	0.007603	3.566101	0.025875
Ground Truth Image (Flower)	0.000272	0.000981	3.805323	0.016489
<i>Fused Image (Flower)</i>	0.000265	0.000889	3.814417	0.016264
Ground Truth Image (Lab)	0.004549	0.038052	3.263459	0.067447
<i>Fused Image (Lab)</i>	0.002534	0.022458	3.338366	0.050344
Ground Truth Image (Leaf)	0.014875	0.074150	2.173367	0.121965
<i>Fused Image (Leaf)</i>	0.000137	0.002177	3.986519	0.011715
Ground Truth Image (Balloon)	0.000779	0.007567	3.514792	0.027906
<i>Fused Image (Balloon)</i>	0.000768	0.007560	3.524006	0.027707
Ground Truth Image (Pepsi)	0.000577	0.003079	3.484715	0.024012
<i>Fused Image (Pepsi)</i>	0.000492	0.002715	3.539362	0.022191
Ground Truth Image (Grass)	0.000388	0.013810	3.876802	0.019686
<i>Fused Image (Grass)</i>	0.001506	0.037708	3.995774	0.038811
Ground Truth Image (Leopard)	0.004786	0.066794	3.694879	0.069181
<i>Fused Image (Leopard)</i>	0.004375	0.063514	3.701540	0.066145
Ground Truth Image (Calendar)	0.002049	0.018711	3.389928	0.045261
<i>Fused Image (Calendar)</i>	0.001496	0.013633	3.442122	0.038680
Ground Truth Image (Flowerpot)	0.000698	0.007647	3.646723	0.026414
<i>Fused Image (Flowerpot)</i>	0.000601	0.006807	3.675266	0.024516
Ground Truth Image (Wine)	0.006612	0.042209	3.036795	0.081314
<i>Fused Image (Wine)</i>	0.000795	0.021114	3.971731	0.028195
Ground Truth Image (Craft)	0.002272	0.007634	2.973879	0.047661
<i>Fused Image (Craft)</i>	0.001930	0.005894	3.028464	0.043926
Ground Truth Image (Remote Sensing)	0.000538	0.001934	3.583163	0.023202
<i>Fused Image (Remote Sensing)</i>	0.000484	0.014062	3.742736	0.021998
Ground Truth Image (medical)	0.055938	0.207243	1.997880	0.236512
<i>Fused Image (medical)</i>	0.010437	0.092595	3.285398	0.102162

Table III. GLCM Mean, GLCM Variance, and GLCM Correlation Statistics Group for Thirty Two Test Images

Image	Statistics Group		
	GLCM Mean	GLCM Variance	GLCM Correlation
Ground Truth Image (Book)	83.549769	3555.095228	0.955341
Fused Image (Book)	85.145989	3612.354769	0.927791
Ground Truth Image (Clock)	98.438408	2618.323182	0.986651
Fused Image (Clock)	99.396485	2583.758708	0.986586
Ground Truth Image (Desk)	98.902152	2193.469902	0.956511
Fused Image (Desk)	100.168962	2258.280262	0.956859
Ground Truth Image (Flower)	104.476057	1447.028130	0.843237
Fused Image (Flower)	109.420958	1480.885899	0.846105
Ground Truth Image (Lab)	123.587088	2267.664020	0.965900
Fused Image (Lab)	124.724426	2255.199243	0.964784
Ground Truth Image (Leaf)	115.470656	1988.845830	0.823525
Fused Image (Leaf)	118.465028	2100.704061	0.826506
Ground Truth Image (Balloon)	114.725061	2338.059838	0.922944
Fused Image (Balloon)	114.719970	2338.258366	0.922642
Ground Truth Image (Pepsi)	98.842437	2033.371791	0.955474
Fused Image (Pepsi)	99.107023	2049.220708	0.954363
Ground Truth Image (Grass)	131.483614	4020.785068	0.949715
Fused Image (Grass)	130.788882	4282.651215	0.872216
Ground Truth Image (Leopard)	93.428679	4318.831815	0.958941
Fused Image (Leopard)	93.405319	4320.231137	0.958685
Ground Truth Image (Calendar)	111.407657	2364.699987	0.873219
Fused Image (Calendar)	112.039722	2390.076632	0.868982
Ground Truth Image (Flowerpot)	105.866240	2709.263116	0.911279
Fused Image (Flowerpot)	110.525997	2765.019730	0.911190
Ground Truth Image (Wine)	118.320718	5034.370333	0.816431
Fused Image (Wine)	118.940819	5090.397991	0.804221
Ground Truth Image (Craft)	140.330169	944.486357	0.921584
Fused Image (Craft)	141.555476	955.488850	0.920787
Ground Truth Image (Remote Sensing)	126.089974	1222.019118	0.898661

Fused Image (remote sensing)	144.970673	1644.400186	0.909464
Ground Truth Image (medical)	67.871419	4782.276431	0.938782
Fused Image (medical)	68.053249	4772.371151	0.933206

Graphical analysis of tested images with respect to ground truth and fused Images are shown below

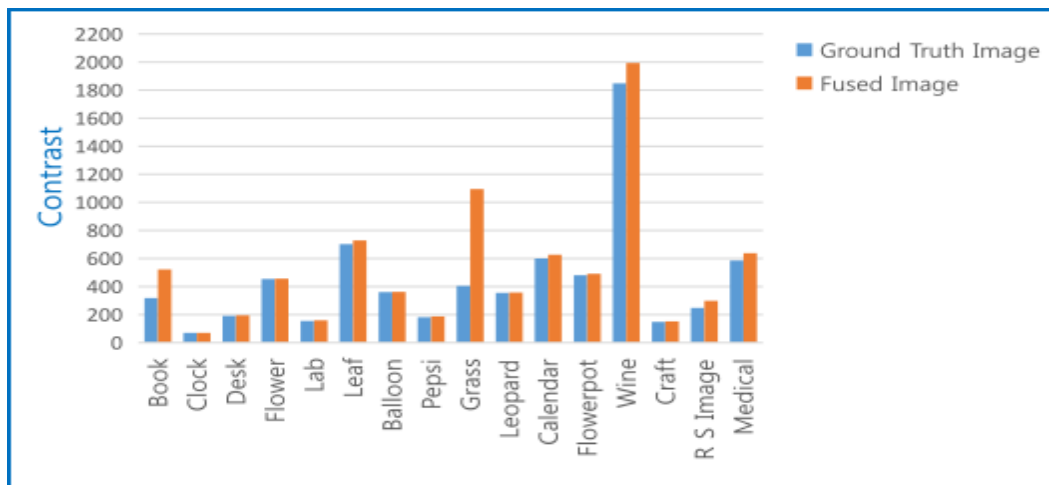


Fig. 4. Texture Metric (Contrast) Comparison between ground truth and fused images

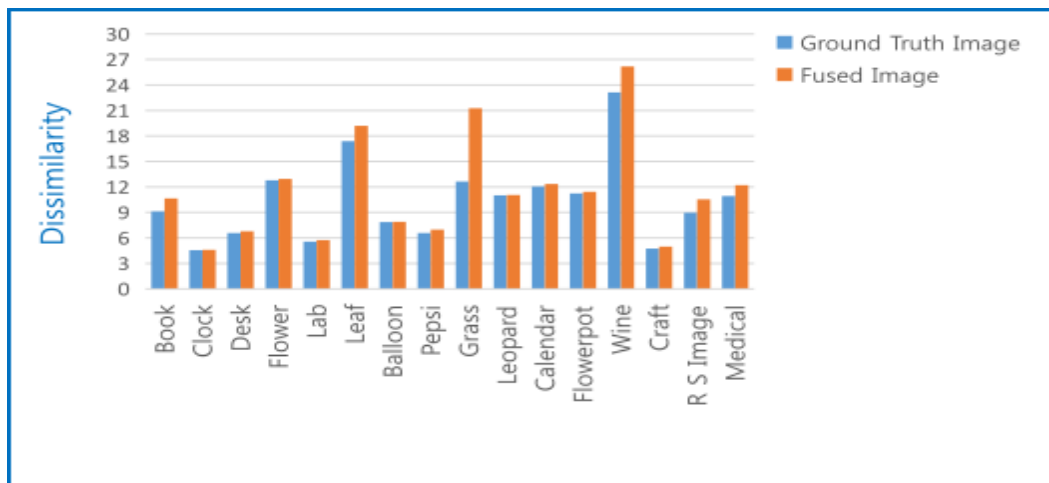


Fig. 5. Texture Metric (Dissimilarity) Comparison between ground truth and fused images

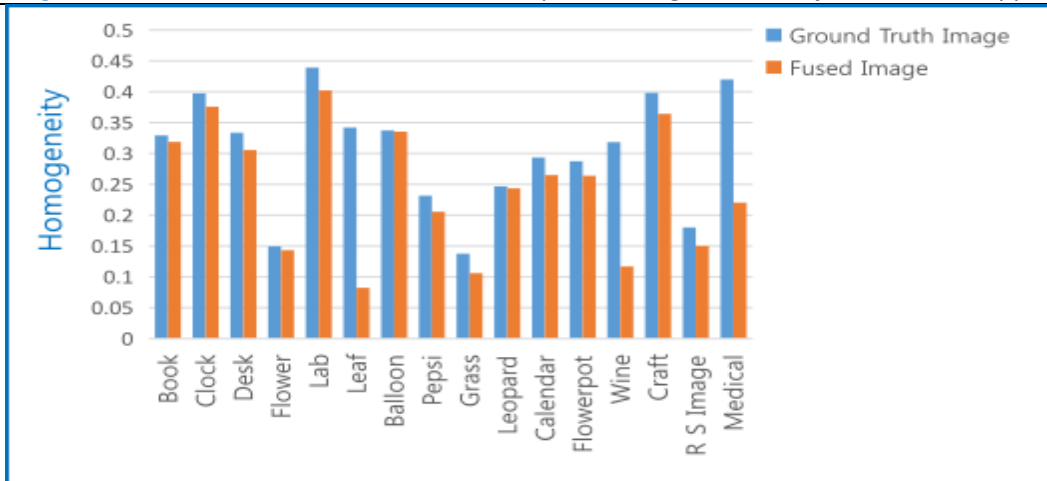


Fig. 6. Texture Metric (Homogeneity) Comparison between ground truth and fused images

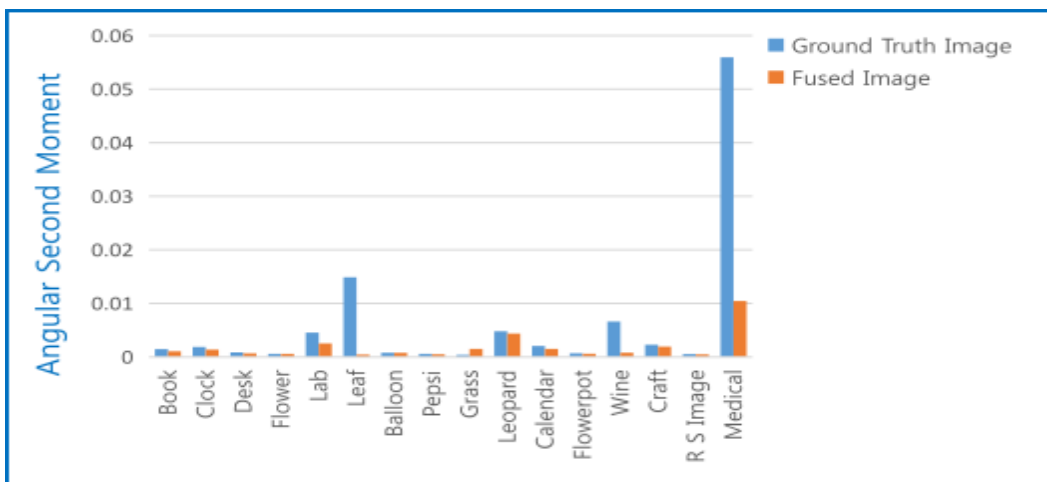


Fig. 7. Texture Metric (Angular Second Moment) Comparison between ground truth and fused images

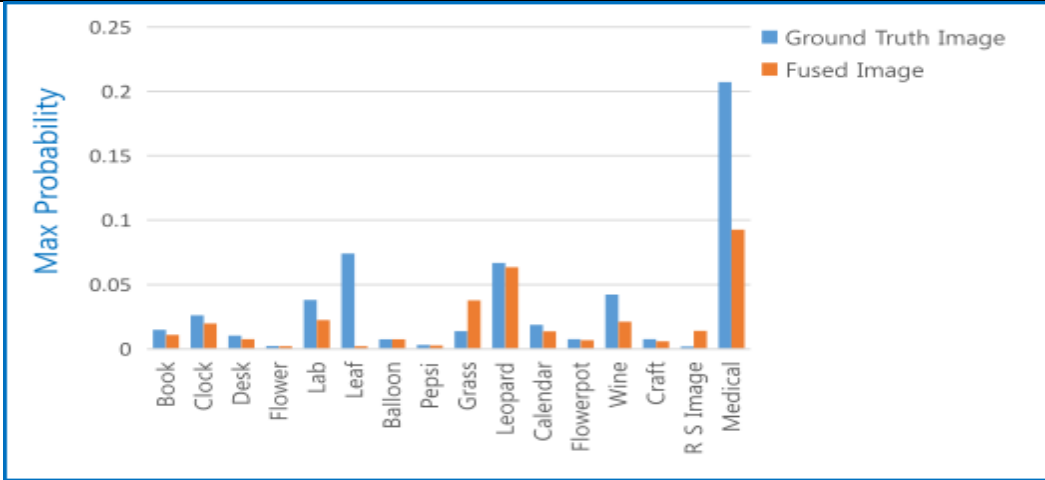


Fig. 8. Texture Metric (Max Probability) Comparison between ground truth and fused images

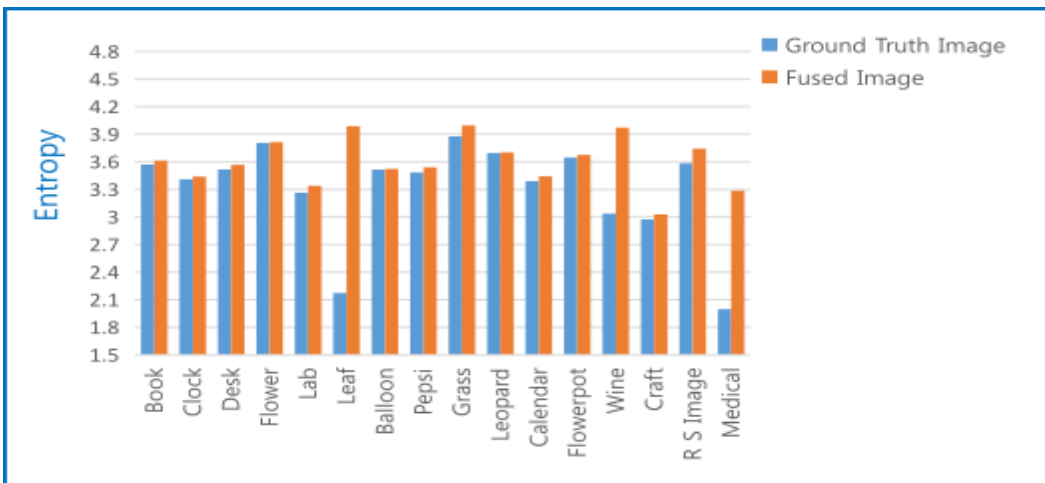


Fig. 9. Texture Metric (Entropy) Comparison between ground truth and fused images

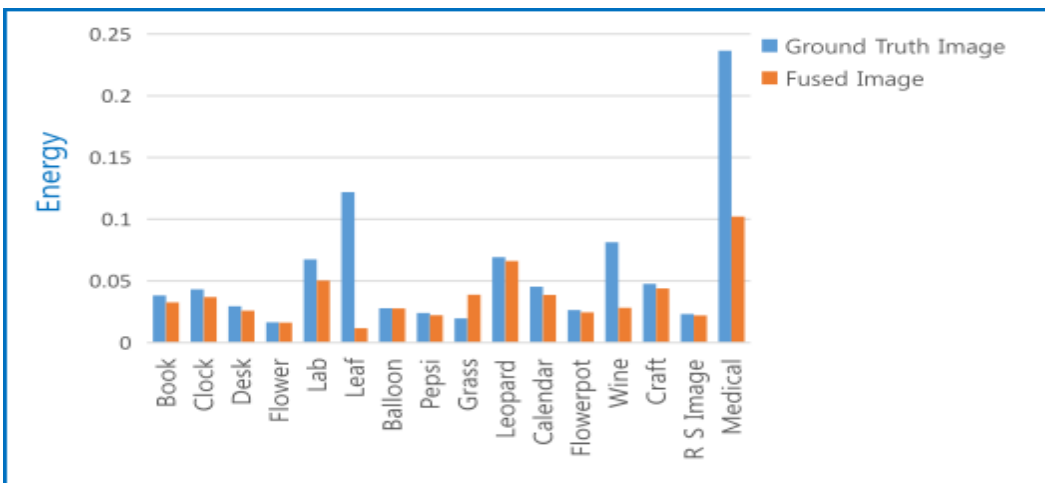


Fig. 10. Texture Metric (Energy) Comparison between ground truth and fused images

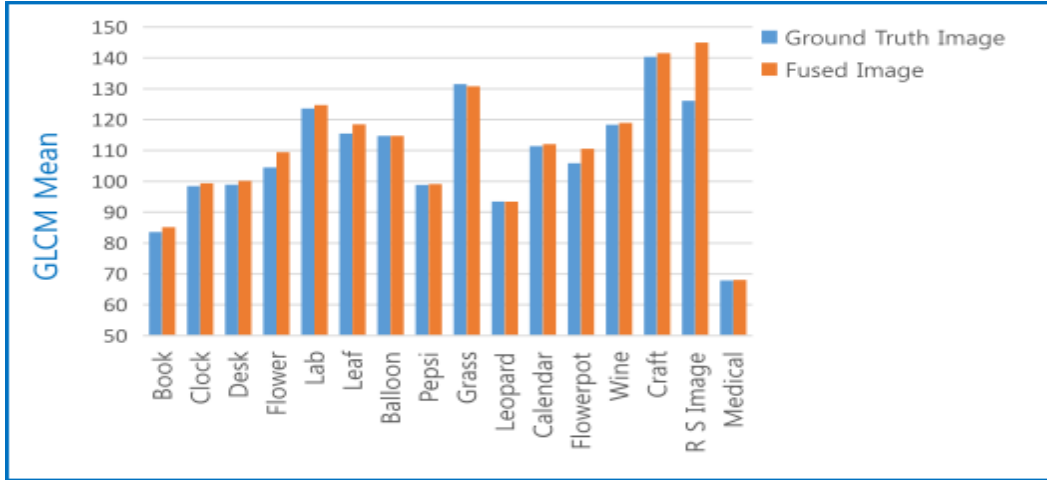


Fig. 11. Texture Metric (GLCM Mean) Comparison between ground truth and fused images

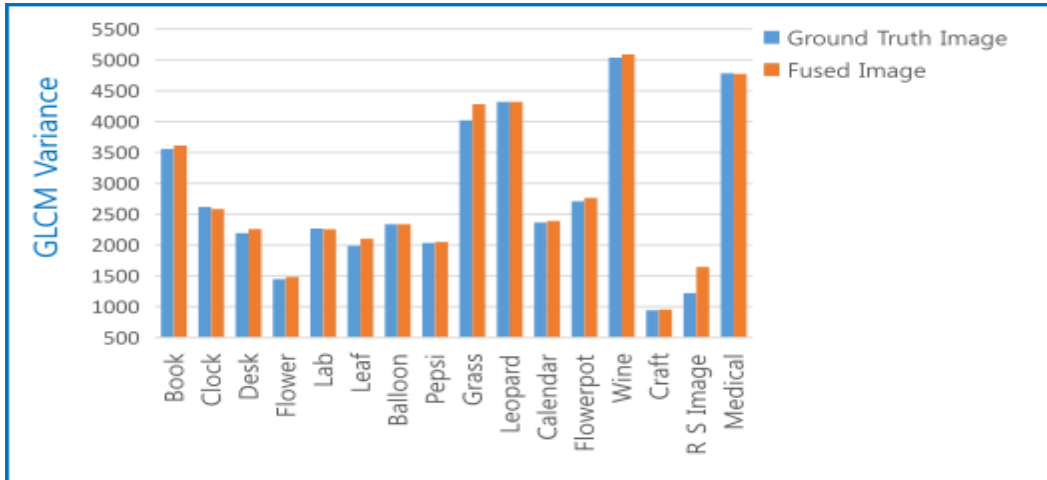


Fig. 12. Texture Metric (GLCM Variance) Comparison between ground truth and fused images

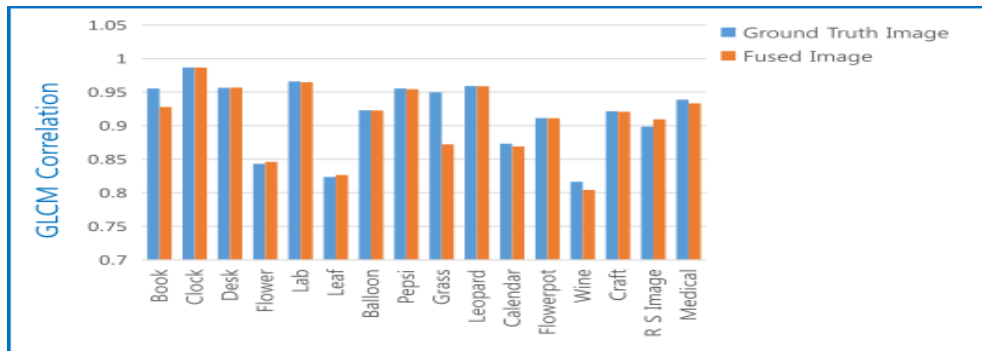


Fig. 13. Texture Metric (GLCM Correlation) Comparison between ground truth and fused images

The main intention of identification of second order statistical measures is to describe entire information of image texture and characteristics of image.

V. Conclusion

The image-based framework and texture analysis method define three groups of invariant features which are treated differently. The first type defines contrast in this group, where parameters like dissimilarity and homogeneity are evaluated. In the second group, parameters like angular second moment, entropy, etc. are evaluated. In the third group, mean, correlation, etc. are evaluated with the data under investigation. Finally, it is concluded that, with respect to the ground truth image, GLCM is the best choice. Further, this work will be enhanced with other methods like Local Binary Pattern (LBP), Auto Correlation Function (ACF), etc.

References

- [1]. Kitada K, Fukuyama K. Land-Use and Land-Cover Mapping Using a Gradable Classification Method. *Remote Sensing*. 2012; 4(6): 1544-1558.
- [2]. Racoviteanu A, Williams MW. Decision Tree and Texture Analysis for Mapping Debris-Covered Glaciers in the Kangchenjunga Area, Eastern Himalaya. *Remote Sensing*. 2012; 4(10): 3078-3109.
- [3]. Garpebring A, Brynolfsson P, Kuess P, et al. Density estimation of grey-level co-occurrence matrices for image texture analysis. *Phys Med Biol*. 2018; 63(19).
- [4]. Rahim M.A., Azam M.S., Hossain N., Islam M.R. Face recognition using local binary patterns (LBP). *Global Journal of Computer Science and Technology*. 2013; 1-12.
- [5]. Kim H. I., Lee S. H., Ro Y. M. Multispectral texture features from visible and near-infrared synthetic face Images for face recognition. *IEEE International Symposium on Multimedia*. 2015; 593-596.
- [6]. Shelton J., Dozier J., Bryant K., Adams J. Genetic based LBP feature extraction and selection for facial recognition. *Proceeding of the 49th Annual Southeast Regional Conference*. 2011; 197-200.
- [7]. Zhang B., Gao Y., Zhao S., Liu J. Local derivative pattern versus local binary pattern: face recognition with high-order local pattern descriptor. *IEEE Transactions on Image Processing*. 2010; 19(2): 533-544.
- [8]. Nagy A.M., Ahmed A., Zayed H. Particle filter based on joint color texture histogram for object tracking. *Proceeding of the First International Conference on Image Processing, Applications and Systems Conference (IPAS)*. 2014; 1-6.
- [9]. Raheja J. L., Kumar S., Chaudhary A. Fabric defect detection based on GLCM and Gabor filter: A comparison. *Optik-International Journal for Light and Electron Optics*. 2013; 124(23): 6469-6474.
- [10]. Patterns M. L. Breast density classification using multiresolution local quinary patterns in Mammograms. *Proceeding of the 21st Annual Conference in Medical Image Understanding and Analysis*. Edinburgh. UK. 2017; 365-376.
- [11]. Rastghalam R, Pourghassem H. Breast cancer detection using MRF-based probable texture feature and decision-level fusion-based classification using HMM on thermography images. *Pattern Recognition*. 2016; 51: 176-186.
- [12]. Duque J. C., Patino J. E., Ruiz L. A., Pardo-Pascual J. E. Measuring intra-urban poverty using land cover and texture metrics derived from remote sensing data. *Landscape and Urban Planning*. 2015; 135: 11-21.
- [13]. Wood E. M., Pidgeon A. M., Radeloff V. C., Keuler N. S. Image texture as a remotely sensed measure of vegetation structure. *Remote Sensing of Environment*. 2012; 121: 516-526.
- [14]. Chinmaya Panigrahy, Ayan Seal, Nihar Kumar Mahato. Fractal dimension based parameter adaptive dual channel PCNN for multi-focus image fusion. *Optics and Lasers in Engineering*. 2020; 133: 106141-106163.
- [15]. Chengfang Zhang. Multifocus image fusion using multiscale transform and convolution sparse representation. *International journal of wavelets, multiresolution and information processing*. 2021; 19(1).
- [16]. Fernandes AFA, Dórea JRR, Rosa GJM. Image Analysis and Computer Vision Applications in Animal Sciences: An Overview. *Front. Vet. Sci*. 2020; 7.
- [17]. Laleh Armi, Shervan Fekri-Ershad. Texture image analysis and texture classification methods - A review. *International Online Journal of Image Processing and Pattern Recognition*. 2019; 2(1): 1-29.
- [18]. Abdul Rasak Zubair, Oluwaseun Adewunmi Alo. Grey Level Co-occurrence Matrix (GLCM) Based Second Order Statistics for Image Texture Analysis. *International Journal of Science and Engineering Investigations*. 2019; 8(93).
- [19]. Manjunath B.S., Ma W.Y. Texture features for browsing and retrieval of image data. *IEEE Transactions on pattern analysis and machine intelligence*. 1996; 18(8): 837-842.
- [20]. Tuceryan M., Jain A.K. Texture analysis, in *Handbook of pattern recognition and computer vision*. World Scientific Publisher. 1993; 235-276.
- [21]. Eichkitz C. G., Davies J., Amtmann J., Schreilechner M.G., De Groot P. Grey level co-occurrence matrix and its application to seismic data. *First Break*. 2015; 33(3): 71-77.
- [22]. Ayushman Ramola, Amit Kumar Shakya, Dai Van Pham. Study of statistical methods for texture analysis and their modern evolutions. *Engineering Reports published by John Wiley & Sons, Ltd.* 2020; 2(1).
- [23]. Orima T, Motoyoshi I. Analysis and Synthesis of Natural Texture Perception From Visual Evoked Potentials. *Front. Neurosci*. 2021; 15.
- [24]. Osapoetra LO, Chan W, Tran W, Kolios MC, Czarnota GJ. Comparison of methods for texture analysis of QUS parametric images in the characterization of breast lesions. *PLoS ONE*. 2020; 15(12).

-
- [25]. Zhang X, Cui J, Wang W, Lin C. A Study for Texture Feature Extraction of High-Resolution Satellite Images Based on a Direction Measure and Gray Level Co-Occurrence Matrix Fusion Algorithm. *Sensors*. 2017; 17(7).
- [26]. Zhi-Kai Huang, Pei-Wu Li, Ling-Ying Hou. Segmentation of textures using PCA fusion based Gray-Level Co-Occurrence Matrix features. *International Conference on Test and Measurement*. 2009; 103-105.